International Journal of Solids and Structures 54 (2015) 12–19

Contents lists available at ScienceDirect

International Journal of Solids and Structures

journal homepage: www.elsevier.com/locate/ijsolstr

On edge chipping in cylindrical surfaces

Herzl Chai *

School of Mechanical Engineering, Faculty of Engineering, Tel Aviv University, Israel

ARTICLE INFO

Article history:
Received 6 December 2013
Received in revised form 22 June 2014
Available online 22 November 2014

Keywords:
Edge chipping
Cylindrical surface
Flint knapping
Teeth
Dental crowns

ABSTRACT

Edge chipping is a basic failure mode in natural, biological and synthetic materials. This work extends earlier studies on edge chipping in orthogonal surfaces to curved ones using solid or hollowed glass cylinders. Vickers indentation is made on the cylindrical surface near a flat edge (Case 1) or on the flat section near the outer (Case 2) or inner (Case 3) cylindrical surface. This brings in a new parameter h/R, the normalized distance from edge. The evolution of damage is observed in-situ using a video camera. For Cases 1 and 2 the chip morphology and chipping load are insensitive to h/R except for Case 2 where the chip becomes narrower as h/R is increased. For Case 3 no surface breaking occurs, although the resulting internal damage may be of concern in applications to opaque materials. A simple analysis is developed which predicts well the effect of surface curvature on chip morphology. The resulting analytical relationships may be applied to such diverse fields as flint knapping, material shaping tools and fracture of mammalian teeth. An interesting aspect of edge chipping is that it facilitates easy means for quantifying fracture toughness in fragile materials. This approach is employed here to as-received silica aerogel cylinders.

© 2014 Elsevier Ltd. All rights reserved.

1. Introduction

Edge chipping is a fracture phenomenon encountered in such diverse fields as flint knapping, common material shaping, tribology, anthropology and dentistry. The earliest application of edge chipping dates back to tool fashioning in early civilizations, typically using blunt-tip stone hammers (Whittaker, 1994). The chip morphology and chipping load are affected by a wealth of variables including indenter's bluntness, stiffness and inclination relative to the contact surface, rate of load transfer, and surface curvature. It is the latter effect which is of main concern here. While orthogonal-surface targets ("Basic" case, Fig. 1a) have received considerable attention (e.g. Almond and McCormick (1990), Quinn et al. (2000), Morrell and Gant (2001), Chai and Lawn (2007a), Petit et al. (2009), Mohajerani and Spelt (2010), Gogotsi et al. (2010)), research on curved surfaces is quite limited. Danzer et al. (2001) studied chipping in a variety of edge shapes, although no analytical relationships for chipping load or chip morphology were offered. This lack of tests and analysis is quite interesting given that edge chipping is a common occurrence in round bodies, e.g. drill bits or end mills (Fang et al., 2001; Liu et al., 2002; De Melo et al., 2006), mammalian teeth (Schubert and Ungar, 2005; Becker and Chamberlain, 2012; Constantino et al., 2010) and dental prosthesis (e.g. Tan et al. (2004), Sailer et al. (2007)). Fig. 2 presents a few examples collected from the literature. As shown, the chip morphology may considerably differ from that in orthogonal surfaces (Fig. 1b).

Beyond the usual interest in material shaping and concerns for structural integrity, edge chipping facilitates a convenient means for evaluating fracture toughness K_C in hard materials (Chai and Lawn, 2007a). Moreover, chip scars on fossil teeth can be used to estimate bite force and, by extension, provide useful insight into diets and evolutionary processes in hominins (Constantino et al., 2010). In this work standard cylindrical glass rods or tubes are used as a simple means for studying the effect of surface curvature on edge chipping. The test pieces are monotonically loaded by a Vickers tool. As shown in Fig. 3, three different configurations are considered: loading on a cylindrical surface a distance h from a flat edge (Case 1) or on a flat section near the outer (Case 2) or inner (Case 3) cylindrical surface. A limited number of tests are also performed on silica aerogel cylinders to assess the applicability of the edge chipping test to the determination of K_C in fragile materials. The evolution of damage is followed by a video camera. The critical load needed to form a chip and the chip dimensions are determined as a function of surface radius R and indent distance h.

Section 2 discusses the experimental apparatus and reviews some relevant analytical relations while Section 3 presents the test results along with some new analytical relations for chip dimensions; the results for the aerogel study are differed to Section 4.3.

---

* Tel.: +972 3 6408342; fax: +972 3 6407617.
E-mail address: herzl@eng.tau.ac.il

http://dx.doi.org/10.1016/j.ijsolstr.2014.11.014
0020-7683/© 2014 Elsevier Ltd. All rights reserved.

In Section 4 the chipping analysis is applied to some cylindrical bodies of interest, e.g. dental crowns, mammalian teeth and aerogel cylinders. The results are discussed in Section 5 and summarized along with major conclusions in Section 6.

2. Materials and methods

The test pieces are made of solid or thick-walled cylindrical tubes cut from standard borosilicate glass rods. As shown in Fig. 3, three different loading configurations are studied, where R and h denote the relevant surface radius and distance between indenter and free surface, respectively. The specimens are placed on a micrometer-controlled stage which allows the indent distance h to be set to within 10–20 μm. The load is applied by a diamond Vickers tool with pyramid corners aligned parallel/normal to a free surface. The test pieces are loaded in a standard loading frame under stroke-control mode at a rate of 0.1 mm min^{-1}. Both R and h are systematically varied. A video camera equipped with a high-power zoom lens is used to monitor the fracture process. The fracture surface is observed by optical microscopy after unloading. The chip dimensions C and D and indent distance h are determined from optical images to within a few μm accuracy.

It is advantageous to review first analytical relationships for the Basic case (Fig. 1) obtained earlier (Chai and Lawn, 2007a). Fracture starts with onset of penny-like median-radial cracks under the contact and continues stably according to the usual indentation relationship $P \sim c^{3/2}$ or

$$P/h^{3/2} = \alpha K_C (c/h)^{3/2}, \tag{1}$$

where P, c and K_C are the load, depth of radial crack and fracture toughness, in that order, and $\alpha K_C = 12.6$ MPa m$^{1/2}$ for soda-lime glass. (A somewhat smaller value for αK_C, 11.9, was reported by Lawn and Fuller (1975)). The constant α in Eq. (1) can be determined once K_C is specified. The latter depends on crack velocity v (Wiederhorn and Bolz, 1970). The crack velocity just prior to onset of chipping was determined from video records as $v = \sim 1$ mm s^{-1}. This yields $K_C = 0.60$ MPa m$^{1/2}$ (Wiederhorn and Bolz, 1970), from which $\alpha = 12.6/0.6 = 21$. From dimensional considerations the ratio c/h at onset of chipping should be fixed so that from Eq. (1) the chipping load is given by

$$P_0 = \beta K_C h^{3/2}, \tag{2}$$

where $\beta = 9.3(1.3)$ independent of material. Eq. (2) offers a simple means to evaluate toughness K_C, where it is only necessary to determine chipping load P_0. The accuracy of the so measured K_C is similar, and perhaps superior, to that determined by more common indentation techniques owing to the fact that the crack front is well removed from the contact site where local damage and plasticity effects occur (Chai and Lawn, 2007a). The chip dimensions in the loading direction, C_0, and transverse to it, D_0 (Fig. 1b) are found to be well approximated by

$$C_0/h = 5.1(1.4), \quad D_0/h = 8(2.4) \tag{3}$$

For the present configurations (Fig. 3) let P_F be the chipping load and C and D the chip dimensions. From non-dimensional considerations one expects the correction to these quantities relative to the orthogonal surface case (Fig. 1a) to be a function of h/R so that from Eqs. (2) and (3)

$$P_F/P_0 = f_F(\underline{h}) \text{ or } P_F/R^{3/2} = \beta K_C \underline{h}^{3/2} f_F(\underline{h}) \tag{4}$$

$$C/C_0 = f_C(\underline{h}) \text{ or } C/R = (C_0/R) f_C(\underline{h}), \quad D/D_0 = f_D(\underline{h}) \text{ or } D/R = (D_0/R) f_D(\underline{h}) \tag{5}$$

$$\underline{h} \equiv h/R, \tag{6}$$

where f_F, f_C and f_D are some functions of $\underline{h}$ which approach unity for $\underline{h} \to 0$.

3. Results

Fig. 4 shows selected frames from three video sequences typifying the fracture behavior for each one of the three configurations studied while Fig. 5 exemplifies the fracture morphology after specimen unloading, as observed on the indented surface (a) and normal to it (b). The fracture conclusively starts with the popping in of damage under the contact (Fig. 4) and follows with growth of two orthogonal, penny-like radial cracks. After some growth the crack running roughly parallel to the surface curls towards the edge. For Cases 1 (a) and 2 (b) the last frame in Fig. 4 just precedes the onset of unstable fracture or chipping while for Case 3 no surface breakage occurs. Instead, as evident from Fig. 5a, the crack front shifts away from the surface and into the specimen interior. Thereafter, stable fracture ensues. Examination of Figs. 1b and 5b reveals that the surface curvature greatly affects chip morphology. For Case 2 elongate chips in the cylinder axis may occur, consistent with some of the chip scars seen in Fig. 2.

3.1. Chipping load

Fig. 6 typifies the crack growth history for each of the three cases studied, where crack length c and load P are normalized according to Eq. (1). The crack first grows monotonically before

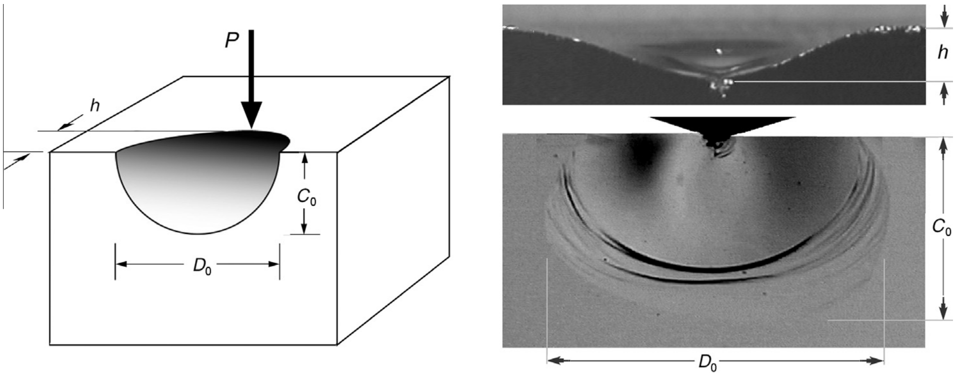

(a) (b)

Fig. 1. Edge chipping in an orthogonal-surface block ("Basic" case) due to Vickers indentation: (a) problem illustration, (b) examples of chips in soda-lime glass test pieces as observed from the contact surface (top) and specimen side (bottom). h denotes indent distance, C_0 and D_0 are chip dimensions. All images are from Chai and Lawn (2007a).

Download English Version:

https://daneshyari.com/en/article/277440

Download Persian Version:

https://daneshyari.com/article/277440

Daneshyari.com